NATIONAL ADVISORY COMMITTEE FOR AERONAUTICS

TECHNICAL NOTE 2577

ON THE ANGULAR DISTRIBUTION OF SLIP LINES IN

POLYCRYSTALLINE ALUMINUM ALLOY

By John M. Hedgepeth, S. B. Batdorf, and J. Lyell Sanders, Jr.

Langley Aeronautical Laboratory
Langley Field, Va.

NACA

Washington

December 1951

NATIONAL ADVISORY COMMITTEE FOR AERONAUTICS

——————

TECHNICAL NOTE 2577

——————

ON THE ANGULAR DISTRIBUTION OF SLIP LINES IN

POLYCRYSTALLINE ALUMINUM ALLOY

By John M. Hedgepeth, S. B. Batdorf, and J. Lyell Sanders, Jr.

SUMMARY

A rather wide distribution in the angular orientation of slip lines
is generally observed in various grains of a metal subjected to plastic
deformation. The relative frequency of occurrence of any given slip line
angle for the case of simple tension has been derived on the basis of a
model of a plastically deforming polycrystal that was recently used as
the basis of a theory of polyaxial stress-strain relations (the so-called
slip theory of plasticity). The results are compared with experiment
and conclusions are drawn as to the limitations of the model.

INTRODUCTION

Theories of plasticity have been of two kinds: physical and mathe-
matical. Physical theories are concerned primarily with the detailed
mechanism of plastic deformation. Mathematical theories, on the other
hand, have as their main objectives the formulation of stress-strain
laws and the application of these laws to the analysis of structures
under load. Most mathematical theories have been formulated on a
phenomenological basis without explicit consideration of the detailed
mechanism of plastic deformation. The formulation of the stress-strain
law of one of the more recent mathematical theories (reference 1),
however, was guided by a consideration of the physical mechanism of
plastic deformation so that it has aspects both of a physical theory
and of a mathematical theory. In this theory - the so-called slip theory
of plasticity - plastic deformation was assumed to be caused by slip
alone and, in the formulation of the stress-strain laws, several addi-
tional assumptions were made (either explicitly or implicitly). In an
effort to check the validity of some of these assumptions a photomicro-
graphic study of the formation of slip lines in polycrystalline aluminum
was made and is discussed in reference 2. The results of that study
gave qualitative indications that the rather idealized model implied in
reference 1 was not strictly correct.

The present study is essentially an extension of the work in reference 2 and represents an attempt to assess quantitatively the adequacy of the model used in reference 1 by examining the statistical distribution of slip angles - those angles which express the orientation of the slip lines. Theoretical distributions are derived on the basis of the model and are compared with an experimental distribution obtained from reference 2.

SYMBOLS

$\bar{N}(\theta)$ probability of a slipped grain having a slip angle less than θ

$S(\theta)$ probability density of slipped grains having a slip angle of θ

θ slip angle (see fig. 1)

θ_{max} maximum slip angle

β angle specifying slip direction (see fig. 2)

β_L value of β for which the resolved shear stress equals the limit shear stress (see fig. 2)

λ, ω spherical coordinates specifying orientation of slip plane (see fig. 1)

$\lambda_1, \lambda_2, \psi$ limits of integration on probability integrals

σ tensile stress

σ_L lowest value of tensile stress to cause slip

τ resolved shear stress

$\bar{\tau}$ maximum value of resolved shear stress on a given slip plane

τ_L limit shear stress

THEORY

Experimental evidence (reference 3) has indicated that, when a single crystal is subjected to a sufficiently high stress, the crystal slips along certain planes in a certain direction in the planes much like a stack of cards. The same action takes place within grains in a polycrystal and can be seen on a polished surface as slip lines which are the intersections of the slip planes with the surface. If a polycrystalline specimen is pulled vertically in uniaxial tension the slip lines will be inclined to the horizontal at various angles designated herein as slip angles. The present investigation is concerned with the relative frequency of occurrence of grains with various slip angles.

The derivation of the angular distribution of slip lines is given in the appendix and is based on the following assumptions (which are common to those used or implied in reference 1):

(1) The crystallographic orientation of the grains in the specimen is random.

(2) Each grain has only one slip system (plane-direction combination).

(3) The microscopic stress state on each grain is the same as the macroscopic stress on the specimen as a whole.

(4) A grain slips when the resolved shear stress in the slip direction in the slip plane is greater than a certain limiting value, herein called the limit shear stress, which is the same for all grains.

On the basis of these assumptions it is shown that the probability of a slipped grain having a slip angle less than a given angle θ is

$$\overline{N}(\theta) = 1 - \frac{2}{\pi} \frac{\displaystyle\int_{\psi}^{\lambda_2} \cos^{-1}\!\left(\frac{\tan\theta}{\tan\lambda}\right)\cos^{-1}\!\left(\frac{\sigma_L}{\sigma\,\sin 2\lambda}\right)\sin\lambda\;d\lambda}{\displaystyle\int_{\lambda_1}^{\lambda_2} \cos^{-1}\!\left(\frac{\sigma_L}{\sigma\,\sin 2\lambda}\right)\sin\lambda\;d\lambda} \tag{1}$$

where the lower limit on the integration ψ is given by

$$\left.\begin{array}{l} \psi = \lambda_1 \quad \text{if} \quad \theta \leq \lambda_1 \\[2mm] \psi = \theta \quad \text{if} \quad \lambda_1 \leq \theta \leq \lambda_2 \\[2mm] \psi = \lambda_2 \quad \text{if} \quad \lambda_2 \leq \theta \end{array}\right\} \tag{2}$$

with

$$\lambda_1 = \frac{1}{2} \sin^{-1} \frac{\sigma_L}{\sigma}$$

$$\lambda_2 = \frac{\pi}{2} - \frac{1}{2} \sin^{-1} \frac{\sigma_L}{\sigma}$$

where the principal value is taken for the inverse sines. The derivative with respect to θ of the expression for $\overline{N}(\theta)$ gives the probability density of slipped grains having a slip angle of θ:

$$S(\theta) = \frac{2 \sec^2 \theta}{\pi} \frac{\displaystyle\int_{\psi}^{\lambda_2} \frac{\cos^{-1}\left(\dfrac{\sigma_L}{\sigma \sin 2\lambda}\right)\sin \lambda \, d\lambda}{\sqrt{\tan^2 \lambda - \tan^2 \theta}}}{\displaystyle\int_{\lambda_1}^{\lambda_2} \cos^{-1}\left(\dfrac{\sigma_L}{\sigma \sin 2\lambda}\right)\sin \lambda \, d\lambda} \tag{3}$$

It should be noted that, although equation (1) constitutes a cumulative frequency, equation (3) represents a frequency distribution.

The functions $\overline{N}$ and S can be viewed as functions of θ with a parametric dependence upon the value of $\frac{\sigma}{\sigma_L}$ which is the ratio between the applied tensile stress and the lowest stress at which slip can occur $\left(\sigma_L = 2\tau_L, \text{ where } \tau_L \text{ is the limit shear stress}\right)$. Attention is called to the fact that, for values of θ greater than λ_2, the density $S(\theta)$ is zero because the limits of integration coincide. Thus, the theory predicts the existence of a maximum angle of slip (equal to λ_2) dependent only on the value of the stress ratio $\frac{\sigma}{\sigma_L}$. The lack of vertical or

near vertical lines on the photomicrograph of a plastically deformed 2S-0 aluminum-alloy specimen shown in figure 3 constitutes experimental confirmation of the existence of a maximum slip angle.

The expression for $\overline{N}(\theta)$ and $S(\theta)$ can be put into a simple closed form for $\frac{\sigma}{\sigma_L} = 1$ by means of limiting processes. Thus,

$$\left.\begin{array}{l} \lim\limits_{\frac{\sigma}{\sigma_L} \longrightarrow 1} \overline{N}(\theta) = \frac{2}{\pi} \sin^{-1} \tan \theta \\[4em] \lim\limits_{\frac{\sigma}{\sigma_L} \longrightarrow 1} S(\theta) = \frac{2}{\pi} \sec \theta \sec 2\theta \end{array}\right\} \qquad (4)$$

For values of $\frac{\sigma}{\sigma_L}$ greater than unity, the formula for $S(\theta)$ can also be put into closed form; however, the resulting expression, which involves elliptic integrals, is so complicated that its use in computations is impractical. For these cases, a more convenient procedure was to perform the integrations in equations (1) and (3) numerically. The resulting curves for $\overline{N}(\theta)$ and $S(\theta)$ are shown in figures 4 and 5, respectively, for three values of the stress ratio $\frac{\sigma}{\sigma_L}$: 1.000 (for which $\theta_{max} = 45^\circ$), 1.156 $\left(\theta_{max} = 60^\circ\right)$, and 2.000 $\left(\theta_{max} = 75^\circ\right)$.

RESULTS AND DISCUSSION

Comparison of Theoretical and Experimental Results

The experimental study reported in reference 2 furnishes experimental data for comparison with the theory of the present paper. A statistical count of observed slip angles was made from one of the photomicrographs in reference 2 (fig. 3) by measuring the slip angle of each slipped grain to the nearest degree and this count is included in table I. This particular photomicrograph was chosen from among those in reference 2 because it contained the largest number of slipped grains and thereby afforded the largest statistical sample.

Inspection of the tabulated distribution of slip angles shows that the distribution is very uneven; the unevenness presumably is attributable to the fact that the statistical sample is not very large. The data, therefore, have been summed cumulatively in table I to determine the number of grains having slip angles between zero and θ. The cumulative sums, divided by the total number of slipped grains, constitute experimental values of $\overline{N}(\theta)$ and are plotted in figure 4 at 5° intervals.

The tensile stress at which the photomicrograph was taken was determined from the measured strain by means of the stress-strain curve of the material. The proper value of σ_L to be used in computing the stress ratio, however, was more difficult to obtain. At first thought, it would seem that σ_L should be taken as the elastic limit (as is done in reference 1), this value yielding a stress ratio of about 5. As is pointed out in reference 2, however, the first slip did not appear in the photomicrographs until the value of the applied tensile stress was much higher than the elastic limit. The results presented in reference 2 indicate that this phenomenon is not necessarily incompatible with the concept that plastic deformation is caused by slip alone; interior grains might be slipping while the surface grains remain elastic (because the surface grains are unsupported on one side and may have a certain degree of hardening introduced by the polishing procedure) and, in addition, the first slips are not visible because of the relatively low resolution of the light microscope. This lag of visible slip can be taken into account by redefining the limit tensile stress σ_L to be the value of σ at which the first visible slip occurs. The use of the new definition is based on the implicit assumption that the corresponding new limit shear stress τ_L, defined as being the value of the resolved shear stress necessary to cause visible slip (see assumption 4), is independent of the crystallographic orientation of the surface grains. On the basis of this new definition of σ_L the resulting experimental stress ratio is about 2.

According to theory, a stress ratio of 2 should produce a maximum slip angle of 75°. The experimental points in figure 4 are in good agreement with the theoretical curve for $\theta_{max} = 60^\circ$ but agree poorly with the theoretical curve for $\theta_{max} = 75^\circ$. This result seems to indicate that the theoretical curves have the proper shape but that the theoretical relationship between stress ratio and maximum slip angle is in error.

The reason for the erroneous theoretical relationship between $\frac{\sigma}{\sigma_L}$ and θ_{max} is connected with the violation of one or more of the four assumptions listed at the beginning of the section entitled "Theory" and with the fact that surface grains do not act as interior ones. A discussion of each assumption and the effect of its violation follows.

Random orientation.- An X-ray diffraction study was made on a specimen similar to that used to obtain the photomicrograph from which the experimental data were derived. The study showed a small amount of crystallographic preferredness. (See fig. 6 for the X-ray diffraction pattern, which was provided through the courtesy of Herbert C. Vacher and the National Bureau of Standards.) The wide disparity between the

theoretical and experimental θ_{max} is difficult to explain on this basis, however, since the effect of the degree of preferredness noted would be merely to change the shape of the probability curve.

Multiplicity of the slip systems.- The assumption of only one slip system is not fulfilled by the material used in the experiment, aluminum, which has a face-centered cubic crystal with 12 slip systems. The slip systems in a face-centered cubic crystal are oriented with respect to each other in a certain definite manner and experimental evidence (see, for example, reference 4) indicates that, when a crystal slips along one system, not only is the operative system strain-hardened but the other latent systems are also strain-hardened to at least the same extent. That the multiplicity of slip systems could have a marked effect on the maximum slip angle can be seen from the following discussion.

One of the consequences of the present theory is that those grains with slip planes almost parallel to the direction of loading will slip only when very high stress ratios are reached. At any finite stress ratio there are always some grains which are still elastic and thus show no slip lines. Consideration of the face-centered cubic crystal shows that, after a certain, as yet undetermined, stress ratio is reached any grain will slip, no matter what its orientation is. Thus, at and above this stress ratio, all the grains exhibit slip lines and the distribution remains frozen. That this stress ratio has already been reached at the strain at which the photomicrograph in figure 3 was taken is evidenced by the lack of unslipped grains in the photomicrograph. The distribution could conceivably have been frozen at a lower stress ratio nearer to the stress ratio theoretically corresponding to the observed experimental θ_{max} (58°).

Homogeneity of microscopic stress.- It is generally agreed that the stress state in a polycrystalline metal varies from grain to grain (see, for example, reference 5). The effect of stress inhomogeneity on the slip angle distribution could be to reduce the maximum slip angle by forcing those grains which would exhibit high slip angles to slip in a different slip system which would produce lower slip angles.

Equality of limit shear stress for various grains.- The results of many single crystal experiments have shown that the value of the limit shear stress is substantially the same for all crystals of the same material. (See, for example, reference 6.) Although it is possible that in a polycrystal there might be a slight random variation of limit shear stress (due the effect of grain boundaries, for instance), the effect of the variation would be to change the shape of the distribution and not to change the relationship between stress ratio based on the first visible slip and maximum slip angle.

Consequences of Present Investigation Relative

to the Slip Theory of Plasticity

Slip-angle distribution, in itself, is only of academic interest.
The main purpose of this investigation is to provide a means of quanti-
tatively checking the basic assumptions of the slip theory of plasticity
in reference 1. The test is rather severe; poor comparisons of slip-
angle distributions do not necessarily mean that the stress-strain rela-
tions, which are the principal objectives, are in serious error. The
test is particularly severe when comparisons of the slip-angle distribu-
tions are made, as in the present paper, at a high strain while the stress-
strain relations are applied mainly at low strain. In addition, the fact
that the characteristic function used in the formulation of the stress-
strain laws is determined empirically entails the consequence that the
effects of stress variation and multiplicity of slip systems are roughly
taken into account. It seems entirely possible, however, on the basis
of the present investigation, that for some types of loading, particularly
in cases involving large strain, the slip theory would be appreciably in
error. If experiments indicate that such is indeed the case, investiga-
tion of the effect that the phenomena discussed in this paper have on
the stress-strain relations predicted by the slip theory would be advis-
able. In particular, a modification of the slip theory by incorporating
the effects of the multiplicity of slip modes of face-centered cubic
crystals should be attempted.

CONCLUDING REMARKS

The comparisons between experimental and calculated slip-angle
distributions based on slip theory indicated good agreement as regards
the general shape of the distributions. The agreement was not so good,
however, between the maximum observed slip angle and the theoretical
maximum slip angle derived from the experimental stress ratio. Of the
four assumptions on which the theoretical derivation was based (random
orientation of grains, single slip system in each grain, stress homo-
geneity, equality of limit shear stress in each grain), the two assump-
tions dealing with the number of slip systems and uniformity of stress
are probably responsible for the disparity between experimental and
theoretical maximum slip angles. If the 12 slip systems characteristic
of face-centered cubic crystals were taken into account, the theory
would be corrected in the right direction as regards maximum slip angle.

If experiments involving arbitrary loading paths should indicate
that the accuracy of the stress-strain relations given by the slip theory

is inadequate, the effects of inhomogeneity of stress and multiplicity
of slip systems on the stress-strain relations should be explored.

Langley Aeronautical Laboratory
　　National Advisory Committee for Aeronautics
　　　　Langley Field, Va., August 20, 1951

APPENDIX

DERIVATION OF SLIP-ANGLE DISTRIBUTION

The orientation of a particular slip plane can be conveniently represented by the coordinates (λ, ω) of the point at which it is tangent to a hemisphere. Because of symmetry only the quarter of the hemisphere shown in figure 1 need be considered.

If the tensile stress σ is applied in the Z-direction as shown in figure 1, the maximum shear stress in the plane tangent at the point $P(\lambda, \omega)$ is given by the formula

$$\bar{\tau} = \frac{\sigma}{2} \sin 2\lambda \tag{A1}$$

The resolved shear stress in this plane in a particular slip direction can be found to be (see fig. 2)

$$\tau = \bar{\tau} \cos \beta \tag{A2}$$

where β is measured from the direction of maximum shear to the slip direction.

A grain with its slip plane tangent at point P will slip if the direction of slip falls within the limits $\pm\beta_L$, where β_L is the angle where $\tau = \tau_L$ or

$$\beta_L = \cos^{-1} \frac{\tau_L}{\bar{\tau}} = \cos^{-1}\left(\frac{\sigma_L}{\sigma \sin 2\lambda}\right) \tag{A3}$$

where $\sigma_L = 2\tau_L$ is the lowest value of the tensile stress to cause slip.

As is well known, slip lines result from the intersection of slip planes and the plane of observation. A plane tangent to the point $P(\lambda, \omega)$ in figure 1 intersects the plane of observation along the observed slip line which is inclined at an angle θ to the horizontal. Slip planes tangent at points along the great circle passing through points B and P produce slip lines that are all inclined to the horizontal at the same angle θ. Solution of the right spherical triangle ABP yields the equation relating the orientation of the grain to its slip angle:

$$\sin \omega = \cot \lambda \tan \theta \tag{A4}$$

Slip can occur along planes which are tangent to the sphere at points in the zone between λ_1 and λ_2, that is, where the maximum shear $\overline{\tau}$ exceeds the limit shear τ_L. The limits λ_1 and λ_2 can be found be replacing $\overline{\tau}$ by τ_L in equation (A1) and are

$$\left.\begin{aligned}
\lambda_1 &= \frac{1}{2} \sin^{-1} \frac{\sigma_L}{\sigma} \\[2mm]
\lambda_2 &= \frac{\pi}{2} - \frac{1}{2} \sin^{-1} \frac{\sigma_L}{\sigma}
\end{aligned}\right\} \tag{A5}$$

The number of grains with slip planes tangent in an area on the sphere $d\Omega$ and slip directions in a sector $d\beta$ is, under the assumption of random orientation,

$$dN' = K \, d\Omega \, d\beta = K \sin \lambda \, d\lambda \, d\omega \, d\beta \tag{A6}$$

where K is a factor of proportionality. The number of slipped grains with slip planes tangent in the area $d\Omega$ is given by

$$dN = \beta_L K \, d\Omega = K \sin \lambda \cos^{-1}\!\left(\frac{\sigma_L}{\sigma \sin 2\lambda}\right) d\lambda \, d\omega \tag{A7}$$

From figure 1 it can be seen that those planes that can produce slip angles with values less than θ are all tangent at points above the great circle passing through B and P. In addition, all slipped grains were found to have slip planes tangent at points within the zone between λ_1 and λ_2. Thus, all slipped grains with slip angles less than θ have planes tangent at points included in the region which is shaded in figure 1. Integration of dN over this shaded region gives the number of slipped grains with slip angles less than θ:

$$N = \frac{\pi K}{2} \int_{\lambda_1}^{\lambda_2} \cos^{-1}\!\left(\frac{\sigma_L}{\sigma \sin 2\lambda}\right) \sin \lambda \, d\lambda -$$

$$K \int_{\psi}^{\lambda_2} \cos^{-1}\!\left(\frac{\tan \theta}{\tan \lambda}\right) \cos^{-1}\!\left(\frac{\sigma_L}{\sigma \sin 2\lambda}\right) \sin \lambda \, d\lambda \tag{A8}$$

where the lower limit ψ is given by

$$\left.\begin{aligned}
\psi &= \lambda_1 \quad \text{if } \theta \leq \lambda_1 \\[2mm]
\psi &= \theta \quad \text{if } \lambda_1 \leq \theta \leq \lambda_2 \\[2mm]
\psi &= \lambda_2 \quad \text{if } \lambda_2 \leq \theta
\end{aligned}\right\} \tag{A9}$$

If the expression for the number of slipped grains with slip angles less than θ is divided by the total number of slipped grains (determined by integrating dN over the whole zone between λ_1 and λ_2), the probability of a slipped grain exhibiting a slip angle less than θ is obtained as

$$\overline{N}(\theta) = 1 - \frac{2}{\pi} \frac{\displaystyle\int_{\psi}^{\lambda_2} \cos^{-1}\!\left(\frac{\tan\theta}{\tan\lambda}\right)\cos^{-1}\!\left(\frac{\sigma_L}{\sigma\sin 2\lambda}\right)\sin\lambda \; d\lambda}{\displaystyle\int_{\lambda_1}^{\lambda_2} \cos^{-1}\!\left(\frac{\sigma_L}{\sigma\sin 2\lambda}\right)\sin\lambda \; d\lambda} \tag{A10}$$

The probability density $S(\theta)$ of slipped grains having slip lines inclined at a given angle θ is given by the derivative of $\overline{N}(\theta)$. The differentiation yields

$$S(\theta) = \frac{2\sec^2\theta}{\pi} \frac{\displaystyle\int_{\psi}^{\lambda_2} \frac{\cos^{-1}\!\left(\frac{\sigma_L}{\sigma\sin 2\lambda}\right)\sin\lambda \; d\lambda}{\sqrt{\tan^2\lambda - \tan^2\theta}}}{\displaystyle\int_{\lambda_1}^{\lambda_2} \cos^{-1}\!\left(\frac{\sigma_L}{\sigma\sin 2\lambda}\right)\sin\lambda \; d\lambda} \tag{A11}$$

Plots of $\overline{N}(\theta)$ and $S(\theta)$ for three values of $\frac{\sigma}{\sigma_L}$ are shown in figures 4 and 5, respectively.

REFERENCES

1. Batdorf, S. B., and Budiansky, Bernard: A Mathematical Theory of
   Plasticity Based on the Concept of Slip. NACA TN 1871, 1949.

2. Johnson, Aldie E., Jr., and Batdorf, S. B.: A Study of Slip Formation
   in Polycrystalline Aluminum. NACA TN 2576, 1951.

3. Seitz, Frederick: The Physics of Metals. McGraw-Hill Book Co., Inc.,
   1943, pp. 73-74.

4. Boas, W.: An Introduction to the Physics of Metals and Alloys.
   John Wiley & Sons, Inc., 1949, p. 78.

5. Boas, W., and Hargreaves, M. E.: On the Inhomogeneity of Plastic
   Deformation in the Crystals of an Aggregate. Proc. Roy. Soc. (London),
   ser. A, vol. 193, no. 1032, April 22, 1948, pp. 89-97.

6. Barrett, Charles S.: Structure of Metals. McGraw-Hill Book Co., Inc.,
   1943, pp. 294-295.

TABLE I.- EXPERIMENTAL SLIP-ANGLE DISTRIBUTION

[2S-0 Aluminum Alloy at 0.022 Strain]

θ (deg)	Grains with slip angle of θ	Cumulative sum	θ (deg)	Grains with slip angle of θ	Cumulative sum
0	1	1	31	2	52
1	1	2	32	5	57
2	0	2	33	2	59
3	1	3	34	2	61
4	1	4	35	7	68
5	1	5	36	4	72
6	0	5	37	3	75
7	2	7	38	2	77
8	1	8	39	5	82
9	2	10	40	3	85
10	1	11	41	3	88
11	1	12	42	3	91
12	1	13	43	4	95
13	0	13	44	3	98
14	2	15	45	2	100
15	3	18	46	2	102
16	0	18	47	3	105
17	3	21	48	3	108
18	1	22	49	4	112
19	3	25	50	2	114
20	1	26	51	0	114
21	2	28	52	2	116
22	2	30	53	2	118
23	3	33	54	0	118
24	5	38	55	0	118
25	3	41	56	2	120
26	1	42	57	2	122
27	1	43	58	1	123
28	0	43			
29	2	45			
30	5	50			
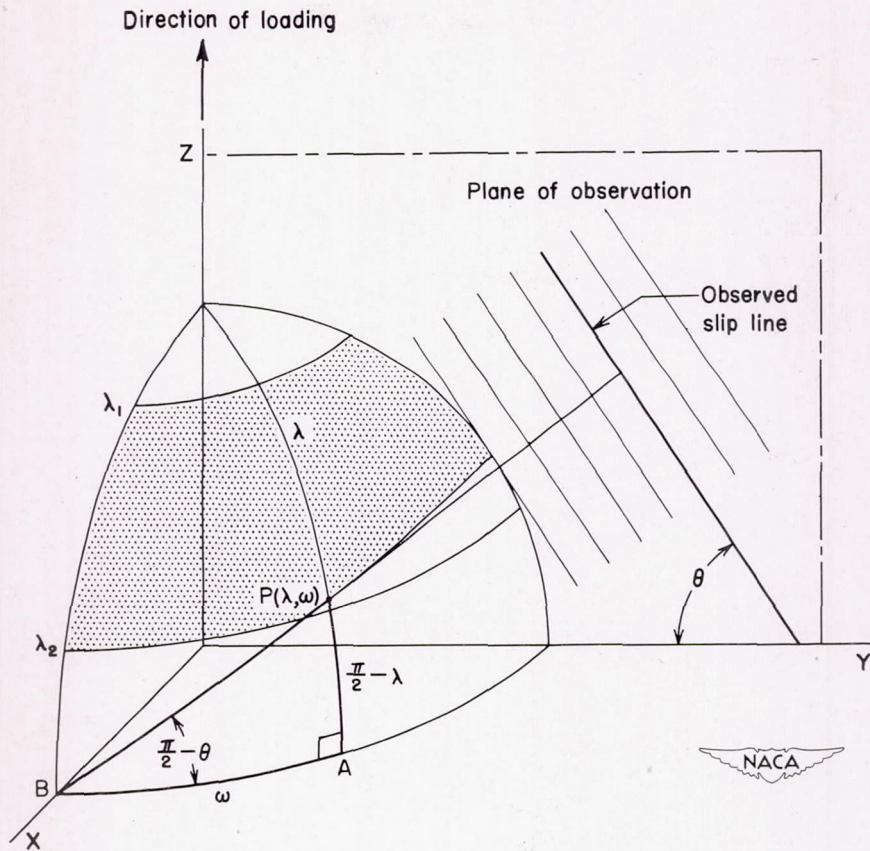
Figure 1.- Portion of unit sphere showing slip-plane orientation, slip angle, and area of integration.
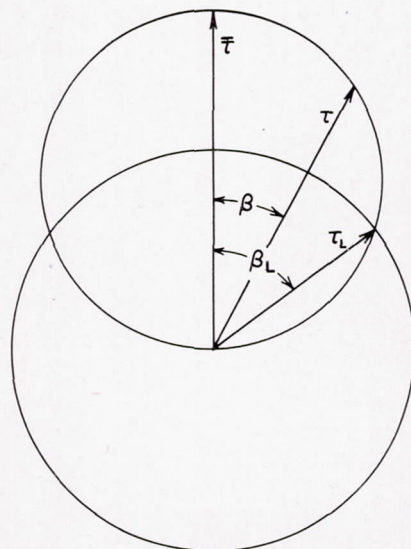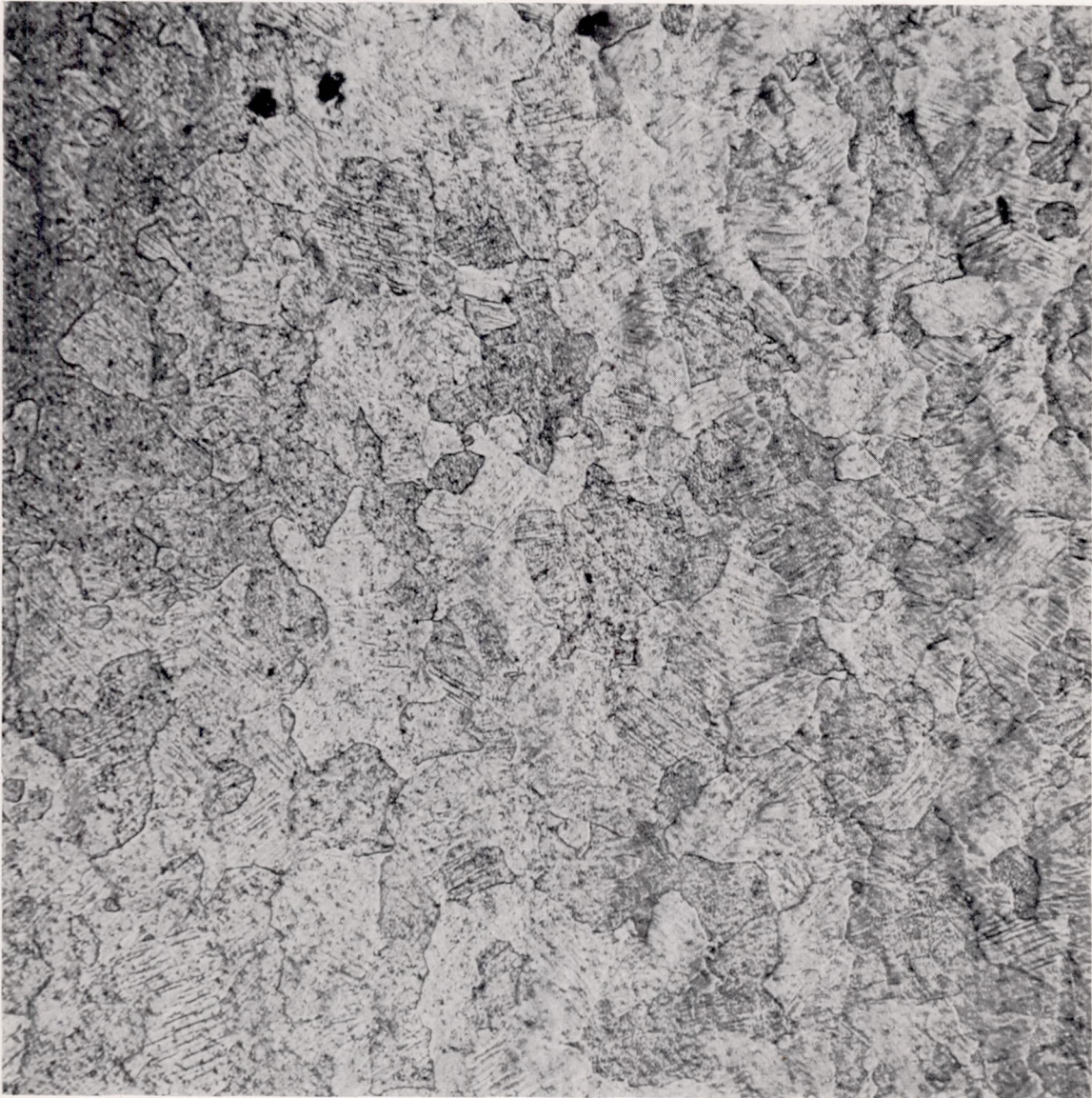

Figure 2.- Resolved shear stress in the slip plane.

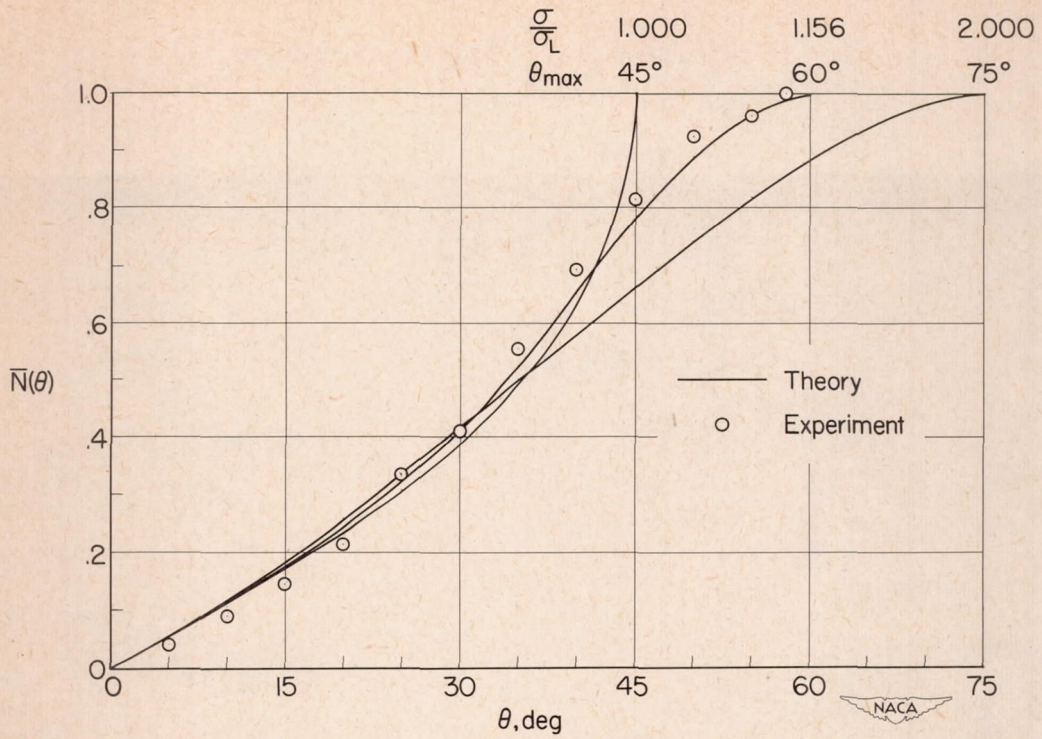Figure 3.- Photomicrograph of 2S-0 aluminum alloy at 0.022 strain. X350.

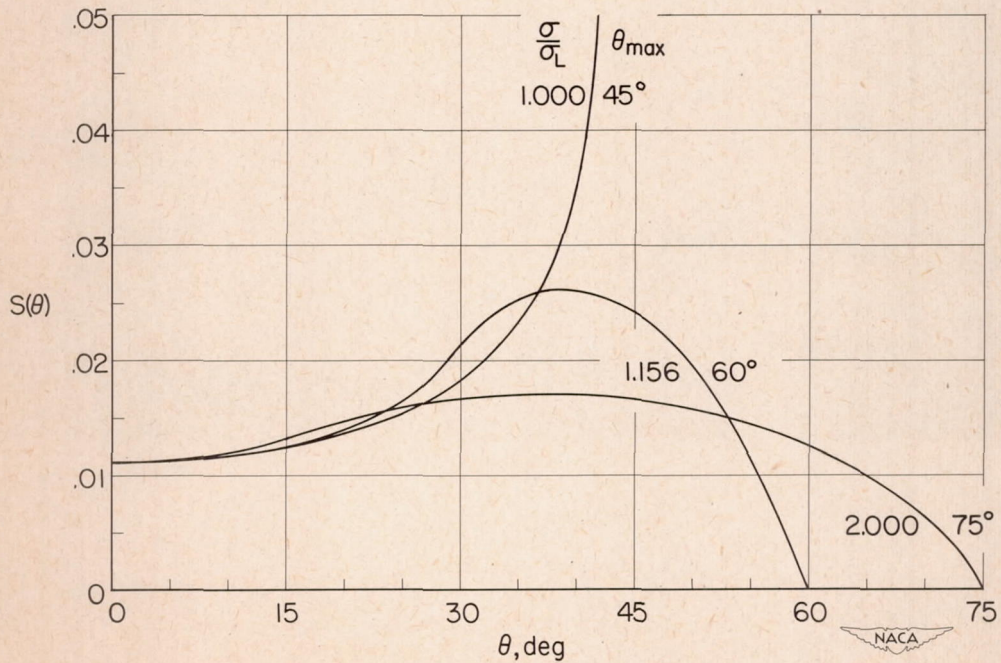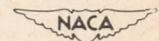Figure 4.- Probability of a slipped grain having a slip angle less than θ.
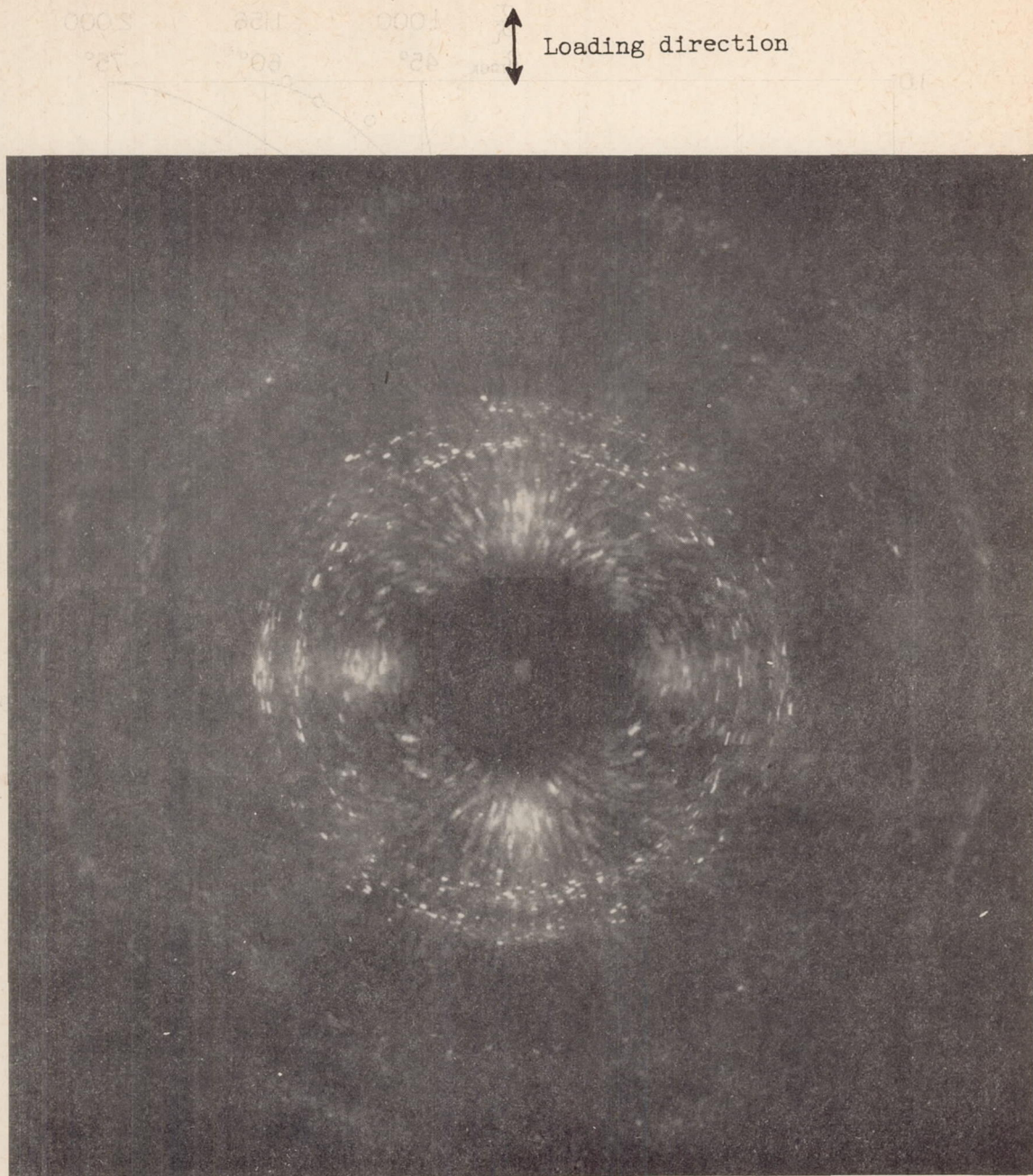
Figure 5.- Theoretical probability density of slipped grains having slip angle of θ.

Loading direction

Figure 6.- X-ray diffraction pattern of 2S-0 aluminum-alloy specimen
before testing. (Mo radiation)